Cement and Concrete Research 42 (2012) 626–632

Contents lists available at SciVerse ScienceDirect

Cement and Concrete Research

journal homepage: http://ees.elsevier.com/CEMCON/default.asp

^{29}Si solid state NMR investigation of pozzolanic reaction occurring in lime-treated Ca-bentonite

Elena Pomakhina [a], Dimitri Deneele [a,b,*], Anne-Claire Gaillot [a], Michael Paris [a], Guy Ouvrard [a]

[a] Institut des Matériaux Jean Rouxel (IMN), Université de Nantes, CNRS, 2 rue de la Houssinière, BP 32229, 44322 Nantes Cedex 3, France
[b] UNAM, IFSTTAR, Institut Français des Sciences et des Technologies des Transports, de l'Aménagement et des Réseaux, BP 4129, route de Bouaye, 44332 Bouguenais, France

ARTICLE INFO

Article history:
Received 24 August 2011
Accepted 31 January 2012

Keywords:
C–S–H (B)
CaO/lime (D)
Pozzolanic reaction (A–D)
NMR spectroscopy (B)
Nucleation and growth

ABSTRACT

Lime is widely used as additive to improve the mechanical properties of natural soil used in earthworks. However, the physico-chemical mechanisms involved are yet not well understood. In order to develop and optimize this treatment method, a better understanding of the interaction between lime and the minerals of the soils, in particular clay minerals, is required. In this study, Ca-bentonite was treated with 2, 5 and 10 wt.% of lime during 1 to 98 days. Modifications in the Si local environment were then monitored by solid state nuclear magnetic resonance to investigate the pozzolanic reaction. All the soil mineral phases contribute to the release of Si and to the pozzolanic reaction, with a rapid and total consumption of Si-polymorph and an exacerbated dissolution of montmorillonite. Mechanism of C–S–H formation, function of the Ca content in the system, was found to match the sorosilicate-tobermorite model described in cement systems.

1. Introduction

Lime stabilization is a widely used means to chemically transform unstable soils into structurally sound construction foundations [1–9]. Lime stabilization is particularly important in road construction for modifying subgrade soils, subbase and base materials. Specifically, lime stabilization modifies a number of important engineering properties of the soils such as a gain in strength, an improved resistance to fracture, fatigue, and permanent deformation, an improved resilient property, a reduced swelling and better resistance to the damaging effects of moisture. The most substantial improvements in these properties are obtained in moderately to highly plastic soils, such as heavy clays. Although lime is generally used to permanently transform fine-grained soils, it may also be used for shorter-term soil modification—for example, to provide a working platform at a construction site.

When quicklime (CaO) is added to a clayey soil, immediate hydration reaction takes place leading to calcium hydroxide ($Ca(OH)_2$) formation. Calcium hydroxide is a reservoir of Ca^{2+} ions that can then be involved into cation exchange in clay mineral interlayer space and/or into sorption on the clay surface leading to a reduction in the thickness of the electrical double layer. These short-term modifications result in a flocculation of clay particles, leading at a macroscopic level to the reduction of the soil plasticity and to significant improvements in the soil workability. Another process, called "long-term stabilization" and involving a pozzolanic reaction, is considered as responsible for the improvement of the mechanical properties of clay. Pozzolanic reaction in general corresponds to the interaction of lime with a silicon-containing material in the presence of water to form a hydrated gel. The reaction is named after the reaction of lime with pozzolana, a volcanic ash which was used by the Romans to make primitive cement. In lime-treated soils, the pozzolanic reaction mechanism is not well understood and existing literature data about long-term stabilization of lime are contradictive and mostly empirical [1,2]. Indeed, few literature data is devoted to the study of the pozzolanic reaction compared to the study of the macroscopic effects of the lime addition (gain in strength, modification of the plasticity, etc.). Concerning the physico-chemical studies, there is a lack of agreement concerning the time-scale over which the reaction take place (lime adsorption and the pozzolanic reaction) and more particularly whether the reaction occur sequentially or occur concurrently. During the past few decades many efforts were devoted to the investigation of the hydraulic reaction in cement and the pozzolanic reaction in composite cement [9–19], for which the solid-state nuclear magnetic resonance (NMR) spectroscopy plays one of the main roles in the investigation of the hydraulic reaction in cement and of the structure of its products, especially calcium silicate hydrate (C–S–H).

The aim of this study is the ^{29}Si solid-state NMR investigation of the specificities of the pozzolanic reaction taking place during the interaction of clay with lime. The montmorillonite clays respond much more rapidly to the lime addition with earlier gain in strength than do kaolinitic clays [1,2], this is why the present investigations were focused on Ca-bentonite, essentially composed of montmorillonite.

* Corresponding author. Tel.: +33 240845802; fax: +33 240845997.
E-mail address: dimitri.deneele@ifsttar.fr (D. Deneele).

0008-8846/$ – see front matter © 2012 Elsevier Ltd. All rights reserved.
doi:10.1016/j.cemconres.2012.01.008

2. Experimental

The studied calcium bentonite (Ca-bentonite) is a natural bentonite purchased from IBECO (sold under the name AGROMONT TH). The study was performed on the fraction below 315 μm, without other purification. The elemental composition determined by ICP-OES is Si (25.6%), Al (9.39%), Fe (1.24%), Mg (2.38%), K (1.79%), Na (0.33%) and Ca (1.48%). A high quality lime (available lime to 95.8% in mass) was used for the bentonite treatment.

In order to investigate the peculiarities of pozzolanic reaction between bentonite and lime, 3 parameters were varied: the concentration of lime, the duration and the temperature of the reaction (20–50 °C). The experiments were carried on a mixture of clay + lime with ultrapure water, with a liquid to solid ratio of 10. In each 10 g solid fraction, 2, 5 and 10 wt.% of lime was added to bentonite. In order to avoid carbonation, we used batch reactor of 125 mL. This way, we reduce the dead volume (100 mL of water + 10 g of solid), and limit the CO_2 uptake. Each time step corresponds to a different batch which was kept close during the duration of the experiment. The pozzolanic reaction being in general considered as a "long-term reaction", the treatment duration was varied from 1 up to 98 days. After each chosen period of time, the reaction was stopped by centrifugation followed by freeze drying and the powder analyzed shortly after. Supernatant solutions were also analyzed by ICP-OES to determine the Ca, Si and Al content in solution.

Solid-state NMR experiments were performed on a Bruker Avance 11.7T (500 MHz ^{1}H frequency) spectrometer with operating frequency on ^{29}Si nuclei of 99.36 MHz, using the magic-angle spinning (MAS) technique. The experimental conditions were performed with mass frequency of 5000 Hz, π/3 excitation pulse and ^{1}H decoupling with r.f. field of 60 kHz. Chemical shift were referred to tetrakis (trimethylsilyl) silane (TMS) as secondary reference ($\delta = -9.8$ ppm from TMS). The spectra were acquired with a recycle delay of 5 and 120 s, since all signals, except silica polymorphs, did not changed in experiment after 5 s. For the silica polymorphs, the signal did not changed in experiment with relaxation delays of 120 s. The number of scans ranged from 2000 up to 36,000. The spectra analysis was performed using the dmfit program [20].

Complementary X-ray diffraction (XRD) analyses were performed on a Bruker AXS D8 Advance with Cu-Kα radiation ($\lambda_{\alpha 1} = 1.54056$ Å) to analyze the mineralogical composition and its evolution in the system. In addition, evolution of Ca speciation in the system was investigated through thermogravimetric analyses (TGA) and differential scanning calorimetry (DSC), carried out with a Setaram TG-DSC 111 apparatus from 25 °C to 830 °C (5 °C/min) under Ar atmosphere to avoid carbonation.

3. Results and discussion

3.1. Initial sample characterization

Calcium bentonite is a natural material containing different clay and non-clay minerals which can influence the bentonite properties and the outcome of the lime treatment. The mineralogy of the initial Ca-bentonite was investigated using multinuclear solid-state NMR. The most informative data were obtained from ^{29}Si MAS NMR (Fig. 1). The main signal with $\delta = -93.3$ ppm is attributed to silicon in montmorillonite [21–23]. Montmorillonite with general formula $(Na,Ca)_{0,3}(Al,Mg)_2Si_4O_{10}(OH)_2 \cdot nH_2O$ is 2:1 layer mineral made of a sheet of octahedrally coordinated aluminum (^{VI}Al in O sheet) between two sheets of corner-sharing silicon tetrahedra (^{IV}Si in T sheets). According to the generally accepted NMR nomenclature, this ^{IV}Si connected to 3 other ^{IV}Si in the T sheet is named Q_3 [24]. The corresponding signal has a rather broad line (half-width at half-height, hwhh ≅ 450 Hz) indicating a local disordering of the Si environment within the montmorillonite structure. This mineral contains a small amount of paramagnetic ions (*e.g.* Fe^{2+}, Fe^{3+}) responsible for an additional broadening of the MAS NMR spectrum and for the absence of signals in the cross-polarization (CP) MAS NMR spectrum (not shown). The lattice relaxation time is less than 1 s for this signal due to the presence of paramagnetic ions. The presence of a small shoulder to the main signal at $\delta \sim -88$ ppm indicates a partial substitution of ^{IV}Si by ^{IV}Al in the T sheet, as commonly found in montmorillonite [22]. As a result, the chemical shift of signals from silicon nuclei located nearby these ^{IV}Al atoms (Q_3(1Al) signal) slightly moves down field.

In the −98 to −112 ppm range, several additional signals of comparatively small intensities can be seen, some of them overlapping those of montmorillonite. The resonances at −100 ppm and −105 ppm are attributed to feldspar $(Na,K)_x(Al_{1+x}Si_{3-x})O_8$ [24–28], the presence of which is confirmed XRD analysis (not shown). The broad resonance in the −109 to −112 ppm region may be considered as a superimposition of signals from Si atoms connected to four other Si (Q_4 signal) in several poorly ordered silicate minerals (SiO_2) such as cristobalite, opal or amorphous silicate [24,29,30]. The presence of cristobalite and opal is confirmed by

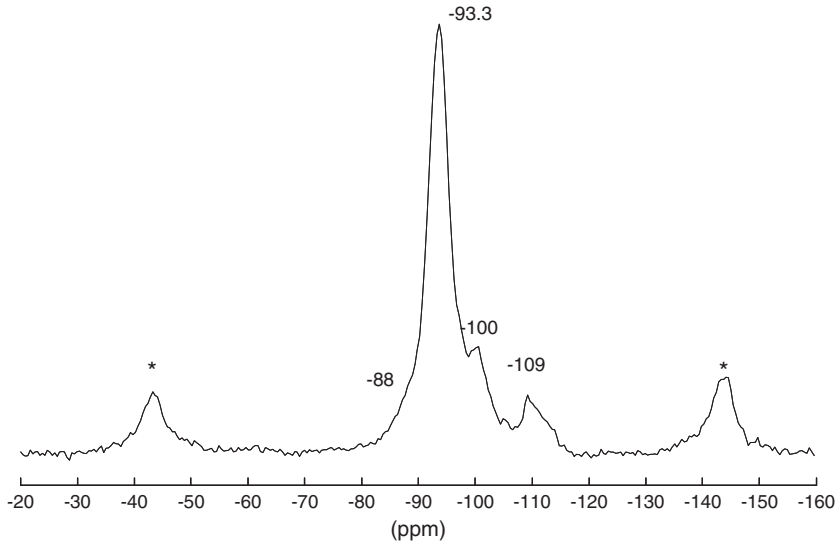

Fig. 1. ^{29}Si MAS NMR spectrum of untreated Ca-bentonite sample. Star symbols indicate spinning side-bands.

XRD (not shown), but the possible occurrence of the other silica polymorphs may be missed due to their disordered structure and comparatively small amount in the sample. In the following, all signals in the −109 to −112 ppm region will therefore simply be referred to as silica polymorphs. Note that, as lattice relaxation times for feldspar and silica polymorphs resonances are far longer than that for the montmorillonite signal, acquisitions with longer time delays were necessary for the former to allow quantification of these phases.

Based on the intensity quantification of the assigned ^{29}Si NMR signals, and the ideal chemical formula of each Si-bearing mineral, the initial Ca-bentonite sample was found to contain mainly montmorillonite (85 wt.%), together with feldspar (10 wt.%) and silica (5 wt.%), the total Si content in the system being estimated to 23 wt.%. This result is in very good agreement with chemical analyses (25 wt.%), despite the 5–10% of error in the silicon content calculation from ^{29}Si MAS NMR spectra due to errors in relative intensities obtained by curve fitting (especially because part of the resonances are partially interfered).

3.2. Bentonite's minerals participation in pozzolanic reaction

Representative ^{29}Si MAS NMR spectra corresponding to various durations of treatment of Ca-bentonite with 10% of lime at room temperature are shown on Fig. 2. In addition to signals found in the initial sample, new signals appear in the −79 to −85 ppm region evolving with the curing time. These signals, based on their chemical shifts, line width and evolution with time and temperature, can be assigned to calcium silicon hydrate (C–S–H) [12,13]. The presence of C–S–H is confirmed by XRD (not shown). In parallel, the resonances from montmorillonite (−93.3 ppm) and feldspar (−100 ppm) observed in the initial bentonite spectrum remain the major signals. Signals from silica polymorph (from −109 to −112 ppm) are still observed in the first period of treatment, but strongly decrease in intensity with time and finally disappear after 28 days of reaction.

Formation of C–S–H phases evidences that pozzolanic reaction does take place in the system when lime is added. Lets then analyze in details the relative reactivity of each Si-bearing minerals in Ca-bentonite. From the rough evolution of the NMR signals given above, silica polymorphs appear to have a high reactivity. To go further and quantify the reactivity of each mineral, quantitative distribution of Si amount among each Si-bearing phase has been calculated for each curing time from integrated intensities of NMR signals (Fig. 3). For this, the total mass content of silicon in the system

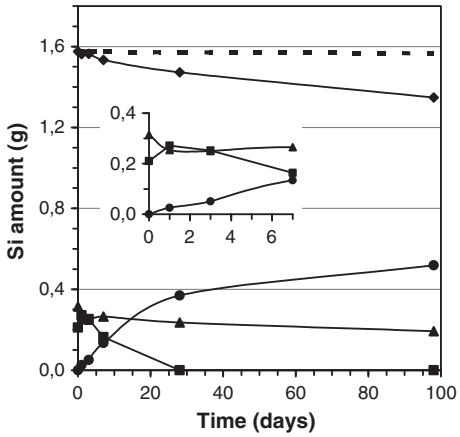

Fig. 3. Time dependence of mass content of silicon from ^{29}Si MAS NMR spectra quantification, involved in each Si-bearing phase of Ca-bentonite treated with 10% of lime at room temperature: C–S–H (circle symbols), silica polymorphs (square symbols), montmorillonite (diamond symbols), feldspar (triangle symbols). The dotted line represents the theoretical montmorillonite dissolution in absence of lime. Inset: zoom of the first week of treatment.

(2.1 g of Si for 9.0 g of bentonite initially introduced in the system) has been used as an external reference. Since the Si concentration measured in solution did not exceed 0.001 g (for 100 mL suspension), the total silicon content in solid phases can be consider as constant. It is found that, though all minerals in bentonite (montmorillonite, feldspar and silica) partly dissolve, the most reactive phases are the silica polymorphs, likely due to their higher solubility.

Further details in their evolution can be assessed. The silica polymorphs content goes through a small maximum after one day of reaction (inset in Fig. 3). The increase of the Q_4 content and the subsequent part of silicon contributing to the formation of silica polymorphs is close to 30% and greater than the amount of Si atoms involved the newly formed C–S–H phases after one day of reaction. This means that, during the first day, the Si conversion from Q_3 into Q_4 environment goes faster than the C–S–H formation. Likely, at the beginning of the reaction, part of silicon is released in solution from some structural defects in montmorillonite and feldspar. This dissolved Si at high pH likely could leads to the precipitation of Si-compound (chalcedony, SiO_2), as suggested by Pozo et al. [31].

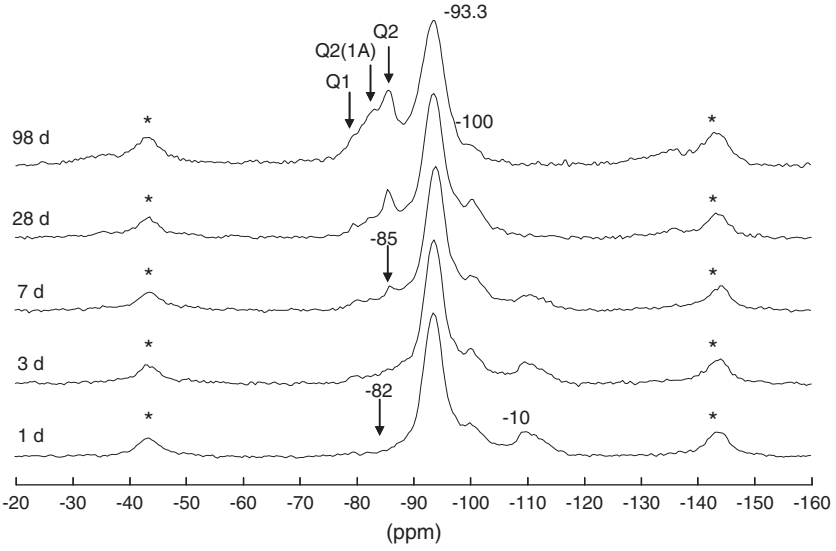

Fig. 2. ^{29}Si MAS NMR spectra of Ca-bentonite treated with 10% of lime at room temperature during 1 to 98 days. Star symbols indicate spinning side-bands.

Both montmorillonite and feldspar are also involved into the pozzolanic reaction. They are sources of Si and Al and their contribution is non negligible: after 98 days of reaction, for the 0.52 g of Si involved in C–S–H, 0.21 g (40%) comes from the initial silica polymorphs while the rest (0.31 g–60%) comes from montmorillonite and feldspar. It is interesting to compare these data of the montmorillonite consumption due to pozzolanic reaction with literature data about montmorillonite dissolution in the same conditions of pH and temperature. Dissolution of montmorillonite in high pH solution was extensively studied, however not in the presence of Ca but in KOH [32,33]. It is reported that the dissolution rate depends on the solution temperature and pH, which in our case varies from 12.5 to 11.7. According to Rozalen [33], smectite dissolution rates for these pH range between 2.14 and 2.88 10^{-14} mol.m^{-2}.s^{-1}. Based on these dissolution rates, theoretical amount of Si remaining in montmorillonite has been estimated (dotted line on Fig. 3). It appears that this amount remains almost constant and higher that experimentally obtained from NMR in the case of bentonite treated with lime. Thus, the rate of Si released from montmorillonite in the presence of Ca is higher than the montmorillonite dissolution rate observed in KOH solution, as mentioned by Leeman et al. [34] since silica is consumed by C–S–H formation until portlandite is consumed.

3.3. C–S–H: review on structure and mechanism of formation

C–S–H structure and composition has long been the topic of many studies. The most accepted structure of C–S–H is similar to tobermorite, [13,35]. Its layered structure contains a calcium plane (that may include additional Ca and water molecules which balance the negative charge of the composite layer) which separates two silicon-aluminum planes made by Si (and Al) dreierketten units. Dreierketten units consist of two Si paired tetrahedra (Q_{2p} sites) linked to a Ca-rich plane and one Si (or Al) bridging tetrahedron (Q_{2br} sites). These units form chains made of 2 ending Q_1 Si and n Q_2 Si-Al sites, where n corresponds to the number of dreierketten units in the chain and can be a measure of the average chain length. However, the tobermorite-like structure of C–S–H does not describe all systems equally well. Some authors consider indeed that C–S–H may sometimes consist of 1, 2 or even 3 different phases (that may coexist at the nanometric scale in an amorphous matrix), the tobermorite-like structure being just one of them [13,36–40]. Tobermorite and related tobermorite-jennite models were mainly developed in the case of systems in the equilibrium state, achieved considering very long reaction times (several weeks or months) and/or elevated temperatures [13,35]. In contrast, to describe the kinetics of C–S–H formation, especially in the first steps of the reaction when the system is far from equilibrium, a two-phase model was proposed by Grutzeck [36,41]. This model is built on two assumptions based on NMR observations [11,12]: 1) two distinct types of C–S–H coexist, one containing dreierketten chains (when the C–S–H structural ratio Ca/Si ≤ 1) and another containing both Si dimers (n = 0) and dreierketten chains (when Ca/Si ≥ 1.1) and 2) the dimeric part of C–S–H is not stable and transforms into dreierketten chains upon reduction of the Ca/Si ratio.

The C–S–H phase made solely of Si dimers has a sorosilicate-like structure [36,41]. The sorosilicate does not have a layer structure like tobermorite, but a 3D one, made of Si paired tetrahedra (dimers) surrounded by Ca polyhedra which hold the structure together. Schematic depiction of sorosilicate-like C–S–H is presented on Fig. 4a (top left). According to Grutzeck, sorosilicate-like C–S–H forms rapidly, almost instantaneously, from dissolved Si and Ca. This phase is stable only in environments having high Ca concentration, with a structural Ca/Si ratio of about 2 or even higher in the first hours of formation. Its stability, however, is relatively limited, and with time and decreasing in Ca content in the media, the sorosilicate may release water, $Ca(OH)_2$ and a certain amount of structural Ca via hydroxyl ion substitution. Decomposition products of sorosilicate depend on the structural Ca/Si ratio. If conditions are favorable (*i.e.* in Ca-rich media maintained over a long period of time, which is not the case in our system), the structural Ca/Si is maintained higher than 1.5 and the sorosilicate phase may transfer into inactive cyclic sorosilicate structure (*e.g.*, tetramer, octamer and or higher). When the Ca/Si ratio reaches 1 however, this sorosilicate structure becomes highly unstable and Si dimers may unzip to form tobermorite-like dreierketten (Fig. 4a). Details in the tobermorite nucleation process remain unclear, but according to Brough et al. [11], chain growth likely proceeds via bridging Si dimers by successive addition of Si or Al tetrahedra to form a pentamer, then an octamer, etc. (Fig. 4b). Growth may also happen by bridging chains together. Defects in the tobermorite structure (discontinuity in the chain) will likely appear during the growth process leading to a distribution of chain lengths in the C–S–H structure. It should be noted that Ca availability is necessary only during the dimers formation step, and sole Si or Al is required for the chain growth (with incorporation of Al into C–S–H structure only observed in the bridging sites — see below). During the tobermorite phase growth, the structural Ca/Si ratio will decrease from 1 to 0.6.

3.4. Kinetics of pozzolanic reaction

In ^{29}Si NMR spectra of Ca-bentonite treated with 10% of lime, the Q_1 Si sites corresponding to chain ends and unconnected C–S–H Si

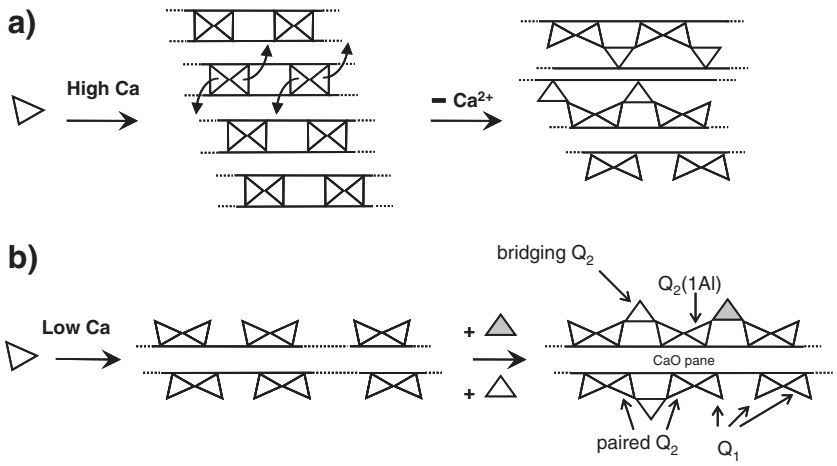

Fig. 4. Mechanism of pozzolanic reaction. (a) Formation of sorosilicate-like phase and transformation to tobermorite; (b) Initial formation of tobermorite dimers followed by dreierketten formation during chain growth. Open and filled triangle represents ^{IV}Si and ^{IV}Al respectively.

dimers are observed immediately after 1 day of reaction (signals with $\delta = -78$ ppm [10,11,18,35] — Fig. 2). Signals corresponding to the C–S–H Q_2 Si sites, in the −84 to −86 ppm range, appear weakly after 1 day of treatment, their intensity increasing considerably after 7 days of treatment. The presence of tetrahedral aluminum in substitution to silicon in the bridging positions of dreierketten chain results in a considerable broadening of the signals from Q_2 sites and the impossibility to distinguish between signals of paired Q_2 (Q_{2p}) and bridging Q_2 (Q_{2br}) Si tetrahedra. The Q_2(1Al) Si sites corresponding to signals around −82 ppm [10,35] are observed for long time treatment (over 28 days).

To analyze the kinetics of the reaction, based on the C–S–H formation mechanism described above (Fig. 4), quantitative evolution of the Si and Al in C–S–H (Q_1 Si and all Q_2 (both Si and Al) sites) as a function of time were extracted from NMR spectra. Because Q_1 Si sites from the sorosilicate and tobermorite structures have the same chemical shift, it is not possible to differentiate these two models. Similarly, it is not possible to distinguish Q_1 Si sites coming from dimers and chain ends. Therefore, the total amount of chains, that is both the sorosilicate dimers and the tobermorite chains (including $n = 0$), hereafter referred to as N_{chain}, correspond to half the amount of Q_1 sites.

Q_2 sites may represent both remaining cyclic sorosilicate phase (forming according to Fig. 4b) and middle dreierketten sites. But since the time reaction during which the solution was rich in Ca was extremely limited, the sorosilicate stabilization into cyclic forms (see above) was assumed to be negligible [41] and Q_2 sites were all assigned to the dreierketten chains sites. The total number of dreierketten units (n_{total}) then corresponds to 1/3 of all Al and Si Q_2 sites ($Q_{2P} + Q_{2br} + 1.5 * Q_2(1Al)$). The averaged chain length (n_{mean}) of C–S–H, calculated in dreierketten units, thus equals n_{total}/N_{chain}. The N_{chain}, n_{total} and n_{mean} values, as well as other useful ones for the following discussion (Ca^{2+} concentration in solution, $Q_1/(Q_1 + Q_2)$ ratio and corresponding structural Ca/Si ratio in C–S–H) are presented in Table 1.

The evolutions of the chain number N_{chain} and of the total number of dreierketten units (n_{total}) as a function of the reaction time are plotted Fig. 5. N_{chain} increases during the first day with an average rate (R_{av}) of about 2.7 10^{-4} mol.day^{-1}, this rate decreasing after only 3 days of treatment, and stabilizes after the first week. Based on these curves, three main periods in the C–S–H formation process can be defined. The first one, during the first 3 days, corresponds to the nucleation of dimers. During this period, the rate of chain growth is rather low ($n_{mean} \cong 0.4–0.5$), with half of the chains being just dimers ($n = 0$), the rest likely limited to pentamers ($n = 1$). Since the Ca concentration is relatively high during that period, we can suppose that most of these dimers likely have the sorosilicate structure. Indeed, $Q_1/(Q_1 + Q_2) \cong 0.6$, which may correspond to a structural Ca/Si ratio in C–S–H around 1.4 [13]. Assuming the two-phase Grutzeck's model, both sorosilicate-like and tobermorite C–S–H structures may then coexist. The second period, from 3 to 28 days of reaction, corresponds to the growth of C–S–H chains. During this period the rate of chain growth is the highest, with an average chain length n_{mean} around 3, while the total number of chains (n_{chain}) stabilizes. After the first three days, the Ca concentration in solution has dropped, while the $Q_1/(Q_1 + Q_2)$ ratio decreased from 0.6 to 0.35 which corresponds to a structural Ca/Si ratio falling down to 1.0. The sorosilicate-like phase would then become highly unstable and transform first into a tobermorite phase (Fig. 4a), which may then grow by successive bridging of dimers to the C–S–H chain (Fig. 4b). Continuous nucleation ensures availability of dimers (Q_1 signal being rather stable). Finally, the third period, between 28 and 98 days of treatment, the growth process continues ($n_{mean} \cong 5$ after 98 days) but is slowing down, and the consumption of dimers is no longer compensated by a nucleation of new ones (decrease in the Q_1 signal). The decrease in the growth and nucleation rate may be then explained by the lower availability of Ca (necessary for the nucleation only) and Si in solution (the silica polymorphs has been totally dissolved after 28 days and montmorillonite and feldspar, which solubility is lower, are less efficient source of Si). During this period $Q_1/(Q_1 + Q_2)$ ratio is around 0.2 and 0.1, the corresponding structural Ca/Si ratio is 0.8–0.7, so that the C–S–H should consist of the tobermorite-like phase only.

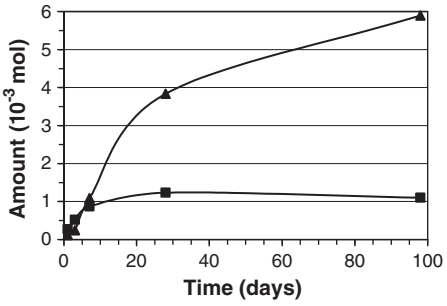

Fig. 5. Time dependence of molar content of total amount of sorosilicate dimers and tobermorite chains N_{chain} (square symbols) and (b) total amount of dreierketten units n_{total} (triangle symbols), extracted from NMR data, for Ca-bentonite treated with 10% of lime at room temperature. 5 10 15 20 25.

3.5. Dependence of Ca content and temperature

The examples of ^{29}Si MAS NMR spectra obtained for treated Ca-bentonite at room temperature with 5% and 2% of lime between 1 and 98 days of treatment are presented on Fig. 6. As for 10%, NMR spectra in the case of lower lime concentration reveal an increase in silica polymorph concentration (Q_4 signal in the −109 to 112 ppm region) in the first days of reaction in comparison with its initial content. It then decreases back, down to complete dissolution in the case of a treatment for 98 days with 5% of lime. Concerning the C–S–H, in the case of 5% of lime the behavior is quite similar to that described for 10% of lime: after one day of treatment the most pronounced signal in ^{29}Si NMR spectrum is the Q_1 resonance, and after 98 days of treatment the relative intensity of the signal from Q_2 sites (including Q_2(1Al) resonance) is the highest, while the intensity of the signal from Q_1 does not change considerably. In the case of 2% of lime only, signals from C–S–H are not easily evidenced due to their lower intensities and to the overlapping of the Q_2 sites signals with that from montmorillonite. Thus, the calculation error in this case is higher than for the other lime content, and only general trends can be drawn.

Table 2 contains values of Ca concentration in solution, $Q_1/(Q_1 + Q_2)$ ratios and corresponding structural Ca/Si ratios for the bentonite treatment with 5% and 2% of lime. As expected, the lower amount of lime added to the system, the faster its consumption. After 1 day of reaction, the Ca content in case of 5% of lime is slightly lower than in case of 10% of lime, but the $Q_1/(Q_1 + Q_2)$ and therefore the corresponding the Ca/Si ratio in C–S–H are the same (1.4). The C–S–H

Table 1
Selected characteristic values of Ca-bentonite treated at 20 ° C with 10% of lime. Ca/Si ratio is deduced by the graphical correlation proposed by Cong and Kirkpatrick [13], from Ca concentration in solution measured by ICP. nmean corresponds to the average chain length.

Curing time (days)	nmean	$[Ca]^{2+}_{sol}$ ($mmol.L^{-1}$)	Q1/(Q1 + Q2)	Structural Ca/Si
1	0.4	17	0.6	1.4
3	0.5	16	0.6	1.4
7	1.3	12	0.35	1.0
28	3.1	0.2	0.2	0.8
98	5.4	0.5	0.1	0.7

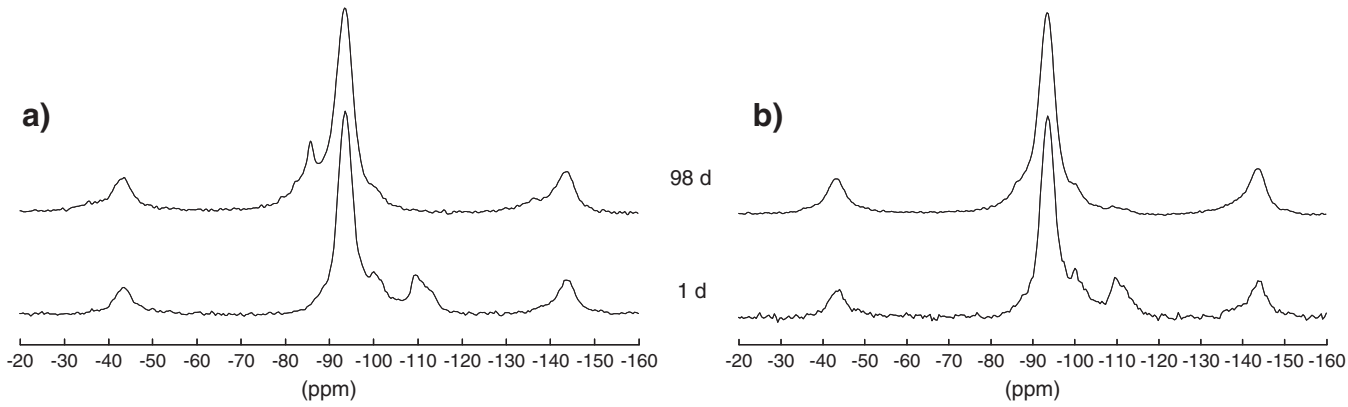

Fig. 6. ^{29}Si MAS NMR spectra of Ca-bentonite treated at room temperature with (a) 5% of lime and (b) 2% of lime during 1 day (bottom spectra) and 98 days (upper spectra).

structure at that moment can likely be described by the two-phase model. However, the C–S–H transformation from sorosilicate to tobermorite occurs quicker, in the first three days (Ca/Si ~1.1). In the case of 2% of lime only, the sorosilicate-like C–S–H may not form, as the $Q_1/(Q_1+Q_2)$ ratio after the first day of treatment is already low (0.2), which corresponds to a C–S–H Ca/Si ratio of ~0.8. The C–S–H structure consists then of tobermorite only with considerably long dreierketten chains with an average chain length n_{mean} of about 3.

Not surprisingly, the final amount of C–S–H is lower for the lower lime addition than in the case of 10% of lime: after 98 days of treatment, the Si contribution in C–S–H is around 0.35 g (~14.4 wt.% of the total Si) and 0.13 g (~5.2 wt.%) for the 5 and 2% lime treatment, respectively (against 0.52 g (~22.6 wt.%) in case of 10% of lime). The modification of the Si contribution in C–S–H (1.5 and 2.7 times increase between 5–10% and 2–5% of lime, respectively) is in good agreement with the difference in the Ca amount initially introduced in the system (2 and 2.5 times higher), taken into account that the final C–S–H Ca/Si ratios are slightly different for the three lime dosages. The total amount of chains N_{chain}, is very limited (less than $5*10^{-5}$ mol) when only 2% of lime is used, and is around 3.10^{-4} mol for 5% of lime, this amount being rather constant during all the treatment duration (from 1 up to 98 days). In comparison, in case of 10% of lime this amount stabilized around 1.10^{-3} mol. This dependence of N_{chain} with the lime concentration could be explained considering that the C–S–H chains mainly grow during the first steps of the process, when probably both types of C–S–H phases are forming. Therefore, the shorter this period, the lower the N_{chain} value. In the same time, the average chain length n_{mean} is longer for both low lime concentrations (excepted for the very beginning when both types of C–S–H structures probably coexist), than for 10% of lime. At the end of longest treatment period for example (98 d), n_{mean} is greater than 10 in case of 5% of lime, against 5.4 only for 10% of lime.

Additional experiments with 2, 5 and 10% of lime were conducted at 50 °C. ^{29}Si MAS NMR spectra obtained for that temperature (not shown) exhibit the same characteristics after 2 days of treatment that what was observed in the case of treatment of 1 month at room temperature (all other conditions being the same). Increasing of curing time then did not lead to significant modification of the spectra. Thus, the temperature increase leads to acceleration of the pozzolanic reaction rates [12] and the previous statement that 2 days of cure at 50 °C corresponds to 4 weeks of treatment at room temperature [42] is confirmed.

4. Conclusions

Lime treatment of Ca-bentonite in presence of water leads on the long term to the formation of secondary phases like C–S–H or C–A–S–H that are commonly found during cement hydration. The pozzolanic reaction that takes place was monitored by 29Si NMR. The evolution of the Si environment revealed the contribution of all Si-based mineral. The high pH ensured by the lime addition and the Ca-rich media favor the montmorillonite dissolution with a higher rate than observed in KOH media for the same pH. Besides, the silica polymorphs are quickly and entirely dissolved after a week (though some precipitation observed during the first step of reaction) providing a complementary source of for the C–S–H precipitation. Its formation mechanism was can well be described by the sorosilicate/tobermorite model, dedicated to the description of C–S–H formation in cement [49, 54]. In the first step of the C–S–H nucleation, with rather high Ca available in the system, both sorosilicate and tobermorite phases may form, with a transformation of the first into the latter when the Ca content in the media decreases. In a second step, growth C–S–H phases may continue even after Ca shortage. This model was found to be valid for treatment of Ca-bentonite with 5 or 10 wt.% of lime while in the case of 2% of lime sole the tobermorite phase likely forms, with a more limited number of chains but of greater length.

Acknowledgments

Nicolas Maubec, Dominique Demare are thanked for performing the lime treatments of the samples, ICP-OES analysis, respectively. EP and DD acknowledge the Région Pays-de-la-Loire (PERLE project) and the French ANR-RGCU research program (TerDouest project) for financial support and LHOIST SA for the supply of lime used.

Table 2
Selected characteristic values of Ca-bentonite treated at 20 ° C with 5 and 2% of lime.

Curing time (days)	n_{mean}	$[Ca]^{2+}_{sol}$ ($mmol.L^{-1}$)	5% of lime $Q_1/(Q_1+Q_2)$	Structural Ca/Si	n_{mean}	$[Ca]^{2+}_{sol}$ ($mmol.L^{-1}$)	2% of lime $Q_1/(Q_1+Q_2)$	Structural Ca/Si
1	2.5	12	0.6	1.4	3.4	2.5	0.2	0.8
3	4.9	8	0.4	1.1	9.9	1.2	0.1	0.7
7	14.6	1.8	0.1	0.7	–	0.6	–	–
28	35.4	0.5	0.06	–	–	0.5	–	–
98	44.6	0.3	0.05	–	–	0.4	–	–

References

[1] F.G. Bell, Lime stabilization of clay minerals and soils, Eng. Geol. 42 (1996) 223–237.
[2] D.I. Boardman, S. Glendinning, C.D.F. Rogers, Development of stabilisation and solidification in lime–clay mixes, Geotechnique 51 (2001) 533–543.
[3] S. Diamond, E.B. Kinter, Mechanisms of soil-lime stabilization. An interpretive review, Highw. Res. Board Rec. 92 (1965) 83–102.
[4] J.L. Eades, R.E. Grim, Reaction of hydrate lime with pure clay minerals in soil stabilization, Highw. Res. Board Bull. 262 (1960) 51–63.
[5] B. Le Runigo, O. Cuisinier, Y.J. Cui, D. Deneele, V. Ferber, Impact of the initial state on fabric and permeability of a lime treated silt under long term leaching, Can. Geotech. J. 46 (2009) 1243–1257.
[6] B. Le Runigo, V. Ferber, Y.J. Cui, O. Cuisinier, D. Deneele, Performance of lime-treated silty soil under long-term hydraulic conditions, Eng. Geol. 118 (2011) 20–28.
[7] S.M. Rao, P. Shivananda, Role of curing temperature in progress of lime soil reactions, Geotech. Geol. Eng. 23 (2005) 79–85.
[8] C.A. Rios, C.D. Williams, M.A. Fullen, Hydrothermal synthesis of hydrogarnet and tobermorite at 175°C from kaolinite and metakaolinite in the $CaO–Al_2O_3–SiO_2–H_2O$ system: a comparative study, Appl. Clay Sci. 43 (2009) 228–237.
[9] C.D.F. Rogers, S. Glendinning, N. Dixon, Lime Stabilization, Thomas Telford, London, 1996.
[10] M.D. Andersen, H.J. Jakobsen, J. Skibsted, Incorporation of aluminum in the calcium silicate hydrate (C–S–H) of hydrated Portland cements: a high-field ^{27}Al and ^{29}Si MAS NMR Investigation, Inorg. Chem. 42 (2003) 2280–2287.
[11] A.R. Brough, C.M. Dobson, I.G. Richardson, G.W. Groves, A study of the pozzolanic reaction by solid-state ^{29}Si nuclear magnetic resonance using selective isotopic enrichment, J. Mater. Sci. 30 (1995) 1671–1678.
[12] A.R. Brough, C.M. Dobson, I.G. Richardson, G.W. Groves, Alkali activation of reactive silica in cements: in situ ^{29}Si MAS NMR studies of the kinetics of silicate polymerization, J. Mater. Sci. 31 (1996) 3365–3373.
[13] X. Cong, R.J. Kirkpatrick, ^{29}Si MAS NMR study of the structure of calcium silicate hydrate, Adv. Cem. Based Mater. 3 (1996) 144–156.
[14] S. Kwan, J. Larosa-Thompson, M.W. Grutzeck, Structures and phase relations of aluminum-substituted calcium silicate hydrate, J. Am. Ceram. Soc. 79 (1996) 967–971.
[15] C.A. Love, I.G. Richardson, A.R. Brough, Composition and structure of C–S–H in white Portland cement-20% metakaolin pastes hydrated at 25°C, Cem. Concr. Res. 37 (2007) 109–117.
[16] F. Méducin, B. Bresson, N. Lequeux, M.-N. de Noirfontaine, H. Zanni, Calcium silicate hydrates investigated by solid-state high resolution ^{1}H and ^{29}Si nuclear magnetic resonance, Cem. Concr. Res. 37 (2007) 631–638.
[17] J. Skibsted, H.J. Jakobsen, C. Hall, Quantification of calcium silicate phases in Portland cements by ^{29}Si MAS NMR spectroscopy, J. Chem. Soc., Faraday Trans. 91 (1995) 4423–4430.
[18] J.F. Young, Investigations of calcium silicate hydrate structure using Silicon-29 nuclear magnetic resonance spectroscopy, J. Am. Ceram. Soc. 71 (1988) C-118–C-120.
[19] H. Zanni, M. Cheyrezy, V. Maret, S. Philippot, P. Nieto, Investigation of hydration and pozzolanic reaction in Reactive Powder Concrete (RPC) using ^{29}Si NMR, Cem. Concr. Res. 26 (1996) 93–100.
[20] D. Massiot, F. Fayon, M. Capron, I. King, S. Le Calvé, B. Alonso, J.-O. Durand, B. Bujoli, Z. Gan, G. Hoatson, Modelling one- and two-dimentional solid-state NMR spectra, Mag. Res. Chem. 40 (2002) 70–76.
[21] R.A. Kinsey, R.J. Kirkpatrick, J. Hower, K.A. Smith, E. Oldfield, High resolution aluminum-27 and silicon-29 nuclear magnetic-resonance spectroscopic study of layer silicates, including clay minerals, Am. Mineral. 70 (1985) 537–548.
[22] J.G. Thompson, ^{29}Si and ^{27}Al nuclear magnetic resonance spectroscopy of 2:1 clay minerals, Clay Miner. 19 (1984) 229–236.
[23] C.A.J. Weiss, S.P. Altaner, R.J. Kirkpatrick, High-resolution ^{29}Si NMR spectroscopy of 2:1 layer silicates: correlations among chemical shift, structural distortions, and chemical variations, Am. Mineral. 72 (1987) 935–942.
[24] E. Lippmaa, M. Magi, A. Samoson, G. Engelhardt, A.-R. Grimmer, Structural studies of silicates by solid-state high-resolution ^{29}Si NMR, J. Am. Chem. Soc. 102 (1980) 4889–4893.
[25] R.J. Kirkpatrick, R.A. Kinsey, K.A. Smith, D.M. Henderson, E. Oldfield, High resolution solid-state sodium-23, aluminum-27, and silicon-29 nuclear magnetic resonance spectroscopic reconnaissance of alkali and plagioclase feldspars, Am. Mineral. 70 (1985) 106–123.
[26] B.L. Phillips, R.J. Kirkpatrick, G.L. Hovis, ^{27}Al, ^{29}Si, and ^{23}Na MAS NMR study of an Al, Si ordered alkali feldspar solid solution series, Phys. Chem. Miner. 16 (1988) 262–275.
[27] B.L. Sherriff, J.S. Hartman, Solid-state high-resolution ^{29}Si NMR of feldspars: Al–Si disorder and the effects of paramagnetic centres, Can. Mineral. 23 (1985) 205–212.
[28] Y.H. Xiao, R.J. Kirkpatrick, R.L. Hay, Y.J. Kim, B.L. Phillips, Investigation of Al, Si order in K-feldspars using ^{27}Al and ^{29}Si MAS NMR, in: NATO Advanced Study Institute — feldspars and their reactions, Mineralogical Society, Edinburgh, Scotland, 1993, pp. 47–61.
[29] H. Graetch, H. Gies, I. Topalovic, NMR, XRD and IR study on microcrystalline opals, Phys. Chem. Miner. 21 (1994) 166–175.
[30] J.V. Smith, B.C. Scott, Nuclear magnetic resonance of silica polymorphs, Nature 303 (1983) 223–225.
[31] C. Pozo, O. Bildstein, J. Raynal, M. Jullien, E. Valcke, Behaviour of silicon release during alteration of nuclear waste glass in compacted clay, Appl. Clay Sci. 35 (2007) 258–267.
[32] F.J. Huertas, C. Caballero, C. Jiménez de Cisneros, F. Huertas, J. Linares, Kinetics of montmorillonite dissolution in granitic solutions, Appl. Geochem. 16 (2001) 397–407.
[33] M.L. Rozalén, F.J. Huertas, P.V. Brady, J. Cama, S. Garcia-Palma, J. Linares, Experimental study of the effect of pH on the kinetics of montmorillonite dissolution at 25 °C, Geochim. Cosmochim. Acta 72 (2008) 4224–4253.
[34] A. Lemann, G. Le Saout, F. Winnefeld, D. Rentsch, B. Lotenbach, Alkali–Silica reaction: the influence of calcium on silica dissolution and the formation of reaction products, J. Am. Ceram. Soc. 94 (4) (2011) 1243–1249.
[35] I.G. Richardson, A.R. Brough, R. Brydson, G.W. Groves, C.M. Dobson, Location of aluminum in substituted calcium silicate hydrate (C–S–H) gels as determined by ^{29}Si and ^{27}Al NMR and EELS, J. Am. Ceram. Soc. 76 (1993) 2285–2288.
[36] M.W. Grutzeck, A new model for the formation of calcium silicate hydrate (C–S–H), Mater. Res. Innovations 3 (1999) 160–170.
[37] A. Nonat, The structure and stoichiometry of C–S–H, Cem. Concr. Res. 34 (2004) 1521–1528.
[38] I.G. Richardson, Tobermorite/jennite- and tobermorite/calcium hydroxide-based models for the structure of C–S–H: applicability to hardened pastes of tricalcium silicate, β-dicalcium silicate, Portland cement, and blends of Portland cement with blast-furnace slag, metakaolin, or silica fume, Cem. Concr. Res. 34 (2004) 1733–1777.
[39] I.G. Richardson, The calcium silicate hydrates, Cem. Concr. Res. 38 (2008) 137–158.
[40] J. Skibsted, C. Hall, Characterization of cement minerals, cements and their reaction products at the atomic and nano scale, Cem. Concr. Res. 38 (2008) 205–225.
[41] M.W. Grutzeck, S. Kwan, J.L. Thompson, A. Benesi, A sorosilicate model for calcium silicate hydrate (C–S–H), J. Mater. Sci. Lett. 18 (1999) 217–220.
[42] D.N. Little, Stabilization of Pavement Subgrades and Base Courses with Lime, National Lime Association, Arlington, 1995.